Evolutionary characterization of pig interferon-inducible transmembrane gene family and member expression dynamics in tracheobronchial lymph nodes of pigs infected with swine respiratory disease viruses

Laura C. Miller, Zhihua Jiang, Yongming Sang, Gregory P. Harhay and Kelly M. Lager

Published Version Information

Citation: Miller, L. C., Jiang, Z., Sang, Y., Harhay, G. P., & Lager, K. M. (2014). Evolutionary characterization of pig interferon-inducible transmembrane gene family and member expression dynamics in tracheobronchial lymph nodes of pigs infected with swine respiratory disease viruses. Veterinary Immunology and Immunopathology, 159(3-4), 180-191.

Digital Object Identifier (DOI): doi:10.1016/j.vetimm.2014.02.015

Publisher's Link: http://www.sciencedirect.com/science/article/pii/S0165242714000518

Evolutionary Characterization of Pig Interferon-inducible Transmembrane Gene Family and Member Expression Dynamics in Tracheobronchial Lymph Nodes of Pigs Infected with Swine Respiratory Disease Viruses

Laura C. Miller*[1], Zhihua Jiang*[2], Yongming Sang*[3], Gregory P. Harhay[4] and Kelly M. Lager[1].

[1]USDA, Agricultural Research Service, National Animal Disease Center, Virus and Prion Research Unit, 1920 Dayton Avenue, Ames, IA 50010, USA; [2]Department of Animal Sciences, Washington State University, Pullman, WA 99164; [3]Department of Anatomy and Physiology, College of Veterinary Medicine, Kansas State University, Manhattan, KS 66506; [4]Animal Health Research Unit, United States Meat Animal Research Center-USDA-ARS, Clay Center, Nebraska 68933

*Co-Corresponding authors. Mailing Addresses: USDA, ARS, National Animal Disease Center, P.O. Box 70, Ames, Iowa 50010-0070; Phone: 515-337-6794, E-mail: laura.miller@ars.usda.gov (L.M.). Department of Animal Sciences, Washington State University, Pullman, WA 99164; Pullman WA 99164–6351; Phone: 509-335-8761, E-mail: jiangz@wsu.edu (Z.J.); Department of Anatomy and Physiology, College of Veterinary Medicine, Kansas State University, Manhattan, KS 66506; Phone: 785-532-4540, E-mail: ysang@vet.k-state.edu (Y.S.)

Running Head: IFITM Evolution in Pigs and SIV-induced member expression dynamics

Abstract

Studies have found that a cluster of duplicated gene loci encoding the interferon-inducible transmembrane proteins (*IFITMs*) family have antiviral activity against several viruses, including influenza A virus. The gene family has 5 and 7 members in humans and mice, respectively. Here, we confirm the current annotation of pig *IFITM1*, *IFITM2*, *IFITM3*, *IFITM5*, *IFITM1L1* and *IFITM1L4*, manually annotated *IFITM1L2, IFITM1L3, IFITM5L, IFITM3L1* and *IFITM3L2,* and provide expressed sequence tag (EST) and/or mRNA evidence, not contained with the NCBI Reference Sequence database (RefSeq), for the existence of *IFITM6*, *IFITM7* and a new *IFITM1*-like (*IFITM1LN*) gene in pigs. Phylogenic analyses showed seven porcine *IFITM* genes with highly conserved human/mouse orthologs known to have anti-viral activity. Digital Gene Expression Tag Profiling (DGETP) of swine tracheobronchial lymph nodes (TBLN) of pigs infected with swine influenza virus (SIV), porcine pseudorabies virus, porcine reproductive and respiratory syndrome virus or porcine circovirus type 2 over 14 days post-inoculation (dpi) showed that gene expression abundance differs dramatically among pig IFITM family members, ranging from 0 to over 3,000 tags per million. In particular, SIV up-regulated *IFITM1* by 5.9 fold at 3 dpi. Bayesian framework further identified pig *IFITM1* and *IFITM3* as differentially expressed genes in the overall transcriptome analysis. In addition to being a component of protein complexes involved in homotypic adhesion, the *IFITM1* is also associated with pathways related to regulation of cell proliferation and *IFITM3* is involved in immune responses.

Keywords: Interferon-inducible transmembrane protein family member, IFITM, Influenza Virus, Swine Genome

1. Introduction

Domestic swine play an important role in human nutrition and economics since pork is the most consumed meat worldwide (http://www.fao.org/ag/againfo/themes/en/meat/backgr_sources.html). Moreover, pigs can harbor a number of zoonotic viruses of which influenza virus is the most important. Understanding how the pig responds to infectious disease may lead to better control of swine diseases that have a significant impact on pork production as well as human health. In addition, learning more about the pig immune response may lead to better animal models to study human disease. Viral respiratory diseases can cause dramatic losses in swine herds and are a major research focus worldwide. Recent advances in technology have enabled the efficient study of gene expression, which can be used to study the molecular pathogenesis and immunology of disease.

Innate antiviral immunity in the mammalian host is orchestrated by the interferon (IFN) system (type I, type II and type III) that plays a cardinal role in early detection and combat of invading viruses through IFN production and action. The interaction of virus and the host IFN-system potentially determines the outcome of most viral diseases (Gonzalez-Navajas et al., 2012; Katze et al., 2008). The interferon-induced transmembrane proteins (IFITMs) are a family of transmembrane proteins that respond differentially to IFN induction and viral infections. The IFITM genes are a subfamily in a larger family of transmembrane proteins called dispanins, which refers to a common two-transmembrane-helix protein structure (Sallman Almen et al., 2012); e.g., IFITM1 has been designated CD225. The current assembly of the human genome (Build 37.3)

indicates there are five *IFITM* family members on chromosome 11: *IFITM1*, *IFITM2*, *IFITM3*, *IFITM5* and IFITM10. The mouse genome has six members: *IFITM1*, *IFITM2*, *IFITM3*, *IFITM5*, *IFITM6* and *IFITM10* located on chromosome 7, and a putative IFITM7 located on chromosome 16. While the multifunctional properties of IFITMs involved in embryo development, cell adhesion/growth and tumor progression are well described (Siegrist et al., 2011), the antiviral activities of IFITMs have only recently been studied. IFITM proteins can confer basal resistance to several viruses and are critical for the virustatic actions of IFN (Brass et al., 2009). Mouse and human IFITM3 expression has been shown to restrict influenza A virus (IAV) replication and IFITM1 and 2 appear to be important in hampering the replication of Marburg and Ebola filoviruses (Everitt et al., 2012; Huang et al., 2011). In addition, IFITM1–3 proteins were found to prevent infection of a growing list of viruses such as HIV-1, SARS, West Nile and Dengue fever (Brass et al., 2009; Everitt et al., 2012; Huang et al., 2011; Lu et al., 2011). Phylogenic analyses show species-specific diverse gene composition and potential functional divergence of vertebrate IFITMs (Hickford et al., 2012; Huang et al., 2011; Siegrist et al., 2011). It is unknown if the duplicated members have virus-specific recognition patterns and signaling pathways.

Our goal was to investigate the regulatory mechanisms and expression patterns of porcine *IFITMs*. In the study reported here, multiple *IFITM* genes were demonstrated to be differentially expressed in tracheobronchial lymph nodes (TBLN) during the course of infection with one of four common viral respiratory pathogens: porcine reproductive and respiratory syndrome virus (PRRSV), swine influenza virus (SIV), porcine circovirus

type 2 (PCV2), and pseudorabies virus (PRV). Additional analyses demonstrated how many putative porcine IFTM family members exist and which are highly conserved human/mouse orthologs that may exert anti-viral activity.

2. Materials and Methods

2.1 Manual annotation and bioinformatic analyses of porcine IFITM family.

Porcine IFITM entries were extracted from the NCBI gene database (http://www.ncbi.nlm.nih.gov/gene/) and further curated using BLASTP against the current swine genome assembly (Sscrofa10.2) (Groenen et al., 2012). The domain structures of IFITM proteins were defined based on human IFITM entries in the Conserved Domain Database (Marchler-Bauer et al., 2013). The sequence alignment and conserved residues were analyzed with Jalview (Waterhouse et al., 2009), and the phylogenic analysis was performed with Mega5 (Tamura et al., 2011). The subcellular location of eukaryotic proteins was predicted using a hybrid approach (Hslpred, http://www.imtech.res.in/raghava/hslpred/) and the algorithms were based on single/multiple sites (Euk-mPloc (Chou and Shen, 2010)) or a decision tree of several support vector machines (MemLoci (Pierleoni et al., 2011)).

2.2 Virus, Animals and Experimental Design

TBLN were collected from pigs that were part of 2 studies of virtually identical design conducted at the National Animal Disease Center (NADC), USDA, ARS, Ames, Iowa. Each study was designed to investigate the comparative global TBLN transcriptome profile of pigs infected with either PRV (Study 1), or SIV, PRRSV, or PCV2 (Study 2).

The experimental design was similar for both studies and TBLN tissue was selected for study because the lymph from the lungs passes through these lymph nodes making them an active site in the immune response against pulmonary disease.

Prior to virus challenge at 4-5 weeks of age, pigs were determined to be free of PRV, SIV, PCV2, and PRRSV. On 0 days-post-inoculation (dpi) pigs received an intranasal challenge with 2 ml of either challenge virus or sham inoculum (control) prepared from the respective cell culture used to propagate challenge viruses. Each group consisted of 20 pigs and was housed in an BSL-2 isolation room from 0-14 dpi, the duration of the experiment. Five pigs from each group both infected and uninfected were euthanized and necropsied on 1, 3, 6 and 14 dpi and TBLN from each pig was collected immediately, minced and stored in RNAlater (Life Technologies Corporation, Grand Island, NY) at -80°C until homogenized for RNA extraction.

Challenge viruses were low passage field isolates used previously at the NADC administered at about 1 x 10^5 $TCID_{50}$ per pig: PRRSV (SDSU73)(Brockmeier et al., 2012), PCV2 (Group 2 European-like)(Lager et al., 2007); SIV (A/SW/OH/511445/2007 H1N1)(Vincent et al., 2009), and PRV (FS268) (Miller et al., 2010).

2.3 Total RNA isolation

TBLN were thawed for homogenization to extract total RNA with MagMAX™-96 for Microarrays Total RNA Isolation Kit (Applied Biosystems, Carlsbad, CA) using the manufacturer's protocol. The integrity of the RNA was confirmed with a 2100

Bioanalyzer and RNA 6000 Nano-chip (Agilent, Santa Clara, CA). The samples used had an average RNA integrity number (RIN) value of 7.8 and 28S:18S rRNA ratio of 1.9. In transcriptome sequencing protocols, it is always advised to use high quality RNA of RIN > 7.

2.4 Digital Gene Expression Tag Profiling

For each necropsy time point, total RNA was pooled for each group to make cDNA libraries for analysis by digital gene expression tag profiling (DGETP). DGETP uses the restriction enzyme, *Dpn*II, to cut 21 bp long sequence tags from each transcript's cDNA, thus expanding the tag-size by at least 7 bp as compared to the predecessor techniques of serial analysis of gene expression (SAGE) and LongSAGE. The longer tag-size allows for a more precise allocation of the tag to the corresponding transcript, because each additional base increases the confidence in the mapping of the tag to a transcript or genomic position.

Tag library preparation was performed at the Iowa State University DNA facility using a DGE-Tag Profiling *Dpn*II Sample Prep kit and protocol (Illumina, Hayward, CA). In brief, total RNA aliquots (1 or 2 μg) were diluted in 50 μL of nuclease-free H_2O and heated at 65°C for 5 min to disrupt secondary structure prior to incubation with magnetic oligo-dT beads to capture the poly-adenlyated RNA fraction. First and second-strand cDNA was synthesized and bead-bound cDNA was subsequently digested with *Dpn*II to retain a cDNA fragment from the most 3‘ GATC to the poly(A)-tail. Unbound cDNA fragments were washed away prior to ligation with the GEX *Dpn*II adapter to the 5’ end

of the bead-bound digested cDNA fragments. This adapter contains a restriction site for *Mme*I which cuts 17 bp downstream from the *Dpn*II site. After subsequent digestion with *Mme*I, 21 bp tags starting with the *Dpn*II recognition sequence were recovered from the beads and dephosphorylated prior to phenol/chloroform extraction. Then, a second adapter (GEX adapter 2) was ligated onto the 3' end of the cDNA tag at the *Mme*I cleavage site. The adapter-ligated cDNA tags were enriched by a 15-cycle PCR amplification using Phusion DNA polymerase (Finnzymes Oy, Illumina-supplied, Hayward, CA) and primers complementary to the adapter sequences. The resulting fragments were purified by excision from a 6% polyacrylamide Tris/Borate/EDTA (TBE) gel.

The DNA was eluted from the gel debris with 1× NEBuffer 2 by gentle rotation for 2 h at room temperature. Gel debris were removed using Spin-X Cellulose Acetate Filter (2 ml, 0.45 μm) and the DNA was precipitated by adding 10 μl of 3 M sodium acetate (pH 5.2) and 325 μl of ethanol (–20°C), followed by centrifugation at 14,000 × g for 20 min. After washing the pellet with 70% ethanol, the DNA was resuspended in 10 μl of 10 mM Tris–HCl, pH8.5 and quantified with a Nanodrop 1000 spectrophotometer. Sequencing using Solexa/Illumina Whole Genome SequencerCluster generation was performed after applying 4 pM of each sample to the individual lanes of an Illumina 1G flowcell. After hybridization of the sequencing primer to the single-stranded products, 18 cycles of base incorporation were carried out on the 1G analyzer according to the manufacturer's instructions. Image analysis and basecalling were performed using the Illumina Pipeline, where sequence tags were obtained after purity filtering.

2.5 Transcriptome determination

First, 64,100 pig mRNA sequences were downloaded from the GenBank database. A Java program was developed to identify the 3' most *Dpn*II cut site, followed by collection of the DGETP tags of 16 nucleotides for each mRNA. By excluding genes/transcripts that had no enzyme cut site and that were potentially repeated entries, we compiled a list of 29,599 genes/transcripts with one tag sequence collected. Second, the unique gene/transcript tags were then used as references to filter each library. Combining the data from the libraries (infected and control) described above revealed that of 29,599 genes/transcripts, 21,144 genes/transcripts were expressed. Third, we used a Bayesian framework approach(Jiang et al., 2013) and determined a total of 1,503 differentially expressed (DE) genes/transcripts among these libraries described above, which were then annotated for orthologs in the human genome against the Refseq database, as the human genome has been well annotated. Lastly, these DE genes were assigned to their associated pathways using the DAVID database (Huang da et al., 2007).

2.6 Quantitative real-time PCR (Q-PCR) analysis

Validation of the results and corroboration of the altered transcript abundance levels were analyzed by real-time reverse transcription-PCR (RT-PCR) on the individual sample of 100 ng total RNA from each pig at each time point. Real-time RT-PCR was done in 25 µl reaction volumes using the SuperScript III Platinum SYBR green One Step qRT-PCR kit (Invitrogen, Carlsbad, CA) according to the supplier's specifications. The *IFITM* primer sets used for this analysis are shown in Table 1. IFN-α_1 (Ss03394862_g1) and IFN-β

(Ss03378485_u1) primers were purchased as Taqman® Custom Probe/Primer sets from Applied Biosystems (Carlsbad, CA). All primers were used at 200 nM. PCR cycling conditions were 50°C for 3 minutes, 95°C for 5 minutes followed by 40 cycles of 95°C for 15 seconds, 60°C for 1 minute, and then, for dissociation curve analysis: 95°C for 15 seconds, 60°C for 15 seconds and 95°C for 15 seconds using an fluorescent thermocycler 7900 (Applied Biosystems, Carlsbad, CA). For real-time PCR, 18S served as the internal control. Relative transcript abundance levels for the other genes were calculated by the $2^{-\Delta\Delta CT}$ method (Livak and Schmittgen, 2001).

3. Results and Discussion

3.1 Structural conservation of pig IFITM family genes

The current assembly of the pig genome (Build 10.2) indicates the presence of 12 potentially functional gene loci in the *IFITM* family (*IFITM1*, *IFITM2*, *IFITM3*, *IFITM1L1*, *IFITM1L2*, *IFITM1L3*, *IFITM1L4*, *IFITM5*, *IFITM5L*, *IFITM3L1*, *IFITM3L2* and *IFITM10*), while humans and mice possess only 5 (*IFITM1*, *IFITM2*, *IFITM3*, *IFITM5* and *IFITM10*) and 7 (*IFITM1*, *IFITM2*, *IFITM3*, *IFITM5*, *IFITM6*, *IFITM7* and *IFITM10*) members, respectively (Figure 1). These loci were manually annotated for validation and to comparatively discover all other *IFITM* family members in pigs using expressed sequence tags (ESTs) and non RefSeq RNA resources, i.e. those outside of the limits of the curated RefSeq database of 21,415 distinct "named" organisms (ftp://ftp.ncbi.nlm.nih.gov/refseq/release/) such as DDBJ/EMBL/GenBank the primary sequence archive, as evidence. The current draft pig genome assembly has 11 *IFITM* family members located on chromosome 2, and 1 member on chromosome 1. The

annotated gene loci, gene symbols, chromosome coordinates, model RefSeq accession numbers and their genomic structures and elements for those porcine *IFITM* family members with EST evidence are detailed in Table 1.

These data raise two questions: 1) how many pig *IFITM* family members would be confirmed with ESTs and/or non RefSeq RNA support as evidence and 2) what is the fate for both IFITM6 and IFITM7 in the pig genome as they are not found in the human genome, but are in the mouse genome? BLAST searches using the model RefSeq sequences of pig *IFITM* family members against both pig EST and non RefSeq RNA databases confirmed the annotation of pig *IFITM1* (XM_003124230.1), *IFITM2* (NM_001246214.1), *IFITM3* (NM_001201382.1), *IFITM5* (XM_003124229.3), *IFITM1L1* (XM_003354415.1) and *IFITM1L4* (XM_003124235.2) (Table 2 and Figure 2). The deduced amino acid sequences indicated two annotated loci (*IFITM1L2*, XM_003354408.1/XM_003354411.1 nd *IFITM5L*, XM_003354416.2) might be annotated duplications as they had the same protein sequences to XM_003354415.1 and XM_003124229.3 (Figure 2). At least three ESTs (HX217039, HX212553 and HX213228) provided evidence for existence of *IFITM6* and one EST (AJ648852) for *IFITM7* in pigs. Several non RefSeq RNA entries (AK234776, AK396508 and AK348267) also supported a new *IFITM1*-like gene (*IFITM1LN*) in the species (Figure 2). However, we did not find any ESTs and/or non RefSeq RNA to support the model RefSeqs for *LOC100621926* (XM_003353647.2), *LOC100627740* (XM_003354422.2) and *LOC100627649* (XM_003354421.1) (Table 2). The continuous gene locus of porcine *IFITM2* was not defined, but the 5'- and 3'-parts of its transcripts (see Fig. 2 for

the ESTs containing the full-length of *IFITM2* coding region) were detected and found to be identical to exon 1 of *IFITM3* and exon 2 of *IFITM1* (or *IFITM1L4*), respectively. We have isolated *IFITM2* cDNA clones from alveolar macrophages that show diverse 3'-regions identical to exons 2 of *IFITM1, IFITM1L2* or *IFITM1L4* genes, respectively, (data not shown). Therefore, there are multiple porcine *IFITM2* variants originating through alternative splicing or exon shuffling. In addition, sequence on an unplaced genomic scaffold (NW_003541064.1, Sscrofa10.2) was found to have 100% identity to the N-terminal ~160 nt of human *IFITM10* (Fig. 1), but no EST evidence was detected for porcine IFITM10.

Our annotation and validation revealed that eight members of pig IFITM family have partial or entire genomic DNA sequences available in two contigs: CU928488.2 and FP565362.1. These members all have a conserved genomic organization: two exons and one intron (Figure 2). The intron regions are completely sequenced for *IFITM1*, *IFITM3*, *IFITM5*, *IFITM1L1* and *IFITM1L4*, and partially sequenced for *IFITM6* and *IFITM1LN*. There are two forms of 3'UTR regions: a long 3'UTR over 1 kb in length and a short 3'UTR less than 250 bp in length. The putative core promoter regions of the porcine *IFITM* genes, except two *IFITM5*-like isoforms, are predicted to contain interferon stimulated response elements (ISRE) (Figure 1 and Table 2).

Although their current nomenclatures are arguable, these members encode proteins that are relatively different in N- and C-terminus regions compared with a highly conserved CD225 superfamily domain that includes one or two transmembrane regions (Figure 3A).

Except for IFITM5 and the tentative IFITM7, other porcine IFITM proteins appear to be combinations with different types of N-terminus regions and C-terminus regions (Figure 2). Phylogenic analysis of all *IFITMs* from humans, mice and pigs shows that *IFITM5* orthologs from the three species form a separate cluster, whereas all other *IFITMs* have evolved from a common ancestor undergoing gene duplication and conversion in each species (Figure 3B) (Hickford et al., 2012; Sallman Almen et al., 2012; Siegrist et al., 2011). Because human *IFITM1-3* and mouse *IFITM3* isoforms have been found to restrict influenza virus replication and infection (Brass et al., 2009; Everitt et al., 2012; Huang et al., 2011), we predict that pigs may have as many as seven *IFITMs* (*IFITM1*, 1L1, 1L2, 1L3, 1L4, 2 and 3) within the *IFITM1-3* cluster (Figure 3B) that potentially exert anti-influenza activity apart from two (CD225-truncated IFITM3L1 and 3L2) that are functionally unknown "mutants". Generally grouped as *IFITMs*, the subcellular localization and membrane integration of *IFITMs* are dynamically regulated by post-translational modifications (PTMs) involving addition of hydrophobic groups for membrane localization (Mann and Jensen, 2003). These PTMs, including myristoylation, palmitoylation and prenylation, could be critical in the regulation of *IFITM* antiviral activity as shown for the S-palmitoylation of human *IFITM3* (Yount et al., 2010). We have identified the predicted conserved cysteine and glycine residues in porcine *IFITMs* (Figure 3A), which are potentially involved in the PTMs for regulation of *IFITM* membrane localization and antiviral activity. We applied three programs for predicting the subcellular location of eukaryotic proteins using a hybrid approach (Hslpred, http://www.imtech.res.in/raghava/hslpred/), the algorithms were based on single/multiple sites (Euk-mPloc (Chou and Shen, 2010)), and a decision tree of several support vector

machines (MemLoci (Pierleoni et al., 2011)). These programs consistently predicted that IFITM5 orthologs are cytoplasmic proteins, while most human or porcine IFITM1-3 isoforms appear to be localized in cytoplasm, cell membrane, mitochondria or secreted into extracellular spaces (Table 3). We conclude that antiviral *IFITMs* should be dynamically regulated through PTMs for their correct sub-cellular location to exert biological, including antiviral, function.

3.2 Clinical evaluation

A comparative study of four swine viral respiratory diseases was completed to evaluate if transcriptome changes in TBLNs were virus-specific, or if they reflected a common response to viral pneumonia regardless of the viral pathogen. PRRSV, PRV, and PCV2 produce a systemic infection in contrast to SIV that primarily infects epithelial tissues in the respiratory tract. However, each virus is capable of replicating in the lung and causing disease therein, the magnitude of which can be dependent on many factors including the viral isolate used. Each virus challenge induced a respiratory disease that resembled what was expected based on experimental and natural infections (as reviewed in (Straw, 1999). Briefly, SIV induced a mild acute clinical disease most apparent between 1 and 3 dpi that was resolving by 14 dpi. The onset of moderate clinical disease in PRRSV- and PRV-infected pigs began 3-6 dpi and was maximal at 14 dpi with some animals beginning convalescence by 14 dpi. In contrast, minimal to no clinical disease or lesions were recognized in PCV2-infected pigs during the experiment. Based on clinical signs, the respiratory disease observed in this study can be separated into an acute response that was resolving by 6 dpi (SIV), a slightly delayed response that developed

maximum lesions by 6 and 14 dpi (PRV and PRRSV) (Brockmeier et al., 2002), and a delayed/minimal response throughout each time-point in the PCV2-infected pigs. In general, for each treatment group a direct relationship was found between virus load and magnitude of disease. For example, in the case of SIV-infected pigs the detection of replicating challenge virus peaked quickly and the pigs had almost cleared the virus by 6 dpi and were negative by 14 dpi. In contrast, the PCV2-infected pigs developed a relatively small virus load throughout the experiment.

3.3 Expression dynamics of pig IFITM family genes

We used TPM (tags per million) values to show basic expression features of pig *IFITM* family members in TBLN of pigs infected with SIV. In addition to SIV, our experiment also involved PRV, PCV2, and PRRSV, plus sham-inoculated controls for comparison. In brief, we made a total of 24 DGETP libraries, including 16 derived from four virus challenges and 8 samples from two sets of control at 1, 3, 6 and 14 dpi. Due to sequence similarity, we found that *IFITM1LN* and *IFITM2*, *IFITM1L4* and *IFITM1LN*, *IFITM3* and *IFITM1L1* shared the 3' most *Dpn*II cut tags: TTTTGAAAAAAAAAAA, TTTTGATGTTGAAAAA and AACATCCGAAGCGAGA, respectively. However, an allelic tag (TTTTAAAAAAAAAAAA) was identified for IFITM2, while unique tags (CTGGGCCTCATTCTGA, AGAAGGTGGCTGGAGA and ACCATCCCCAGGGAGA) were found for IFITM1, IFITM5 and IFITM6, respectively. As the tentative *IFITM7* has an incomplete cDNA sequence, we excluded it in the analysis. These tag sequences can be found in the mRNA sequences listed in Figure 2. The validity and kinetics of transcript abundance of *IFITM1*, *IFITM1L1*, *IFITM1L2*,

IFITM1L3, *IFITM1L4*, *IFITM2*, *IFITM3*, *IFITM3L1*, *IFITM3L2* and *IFITM5* were evaluated using real-time RT-PCR (Fig. 5). Regardless of the member ambiguities caused by sequence similarity between IFITM members in Figure 4, the expression dynamics of IFITM1, IFITM2, IFITM3, IFITM1L1 and IFITM1L4 were similarly examined using both DGETP and RT-PCR, and were found to be consistent, particularly in the tissues infected with SIV, PRV and PCV2. However, the expression dynamics of IFITM family members in PRRSV-infected tissues showed different profiles between the two quantitative techniques, i.e. earlier stimulation in DGETP in contrast to the latter stimulation in the RT-PCR assays. This may require further investigation.

The abundance of gene expression in the present study is quite different among the pig *IFITM* family members regardless of virus. As shown in Figure 4 in the DGETP data, *IFITM2*, *IFITM1L4*, *IFITM1LN* and *IFITM6* seem abundantly expressed, but none expressed more than 400 TPM per library. However, expression of IFITM1 and IFITM3/IFITM1L1 increased in response to infection dramatically, with instances reaching over 3,000 TPM per sample (Figure 4). We also noted that the relative abundance of gene expression detected was quite different among the DGETP and RT-PCR data (Figure 4 and 5) as seen in other studies the DGETP method often produced higher transcript ratios (in either direction) than real-time quantitative RT-PCR (David et al., 2010). (Liu et al., 2011) also observed a systematic bias for RNA-Seq in the analysis of genes with relatively low expression levels. Specifically, DEGs missed by RNA-Seq (i.e. false negatives) were characterized by low expression levels in the examined samples, as indicated by lower RNA-Seq read counts and higher raw C_t values by real-

time qPCR. While the expression levels of IFITM1 and IFITM3/IFITM1L1 had 10-100 fold higher expression than others in the DGETP data (Figure 4), the gene-specific RT-PCR analysis showed more uniform expression abundance among different IFITM members, except IFITM2 that had the highest expression particularly at 3 dpi of PRV infection. Considering that the DGETP analyses probably assigned multiple IFITM1-like (including IFITM1 and IFITM1L1-1L4) and IFITM3-like (including IFITM3 and IFITM3L1-3L2) homologs under IFITM1 and IFITM3, the higher abundance of IFITM1 and IFITM3 in DGETP data was understandable. In addition, *IFITM5* was expressed at low levels in porcine TBLN, as the DGETP analysis TPM ranged from 0 to 1.2 in both virus-challenged samples and controls and in RT-PCR there was no noticeable fold change from control in the virus-infected samples. As shown in Table 2, *IFITM5* does not contain an interferon stimulated response element (ISRE) in its promoter region indicating the gene is not interferon inducible. Therefore, it does not surprise us that expression of the pig IFITM5 was not induced by virus.

Gene expression response timing depends on the type of virus. As illustrated in Figure 4, the IFITM family members responded to SIV infection relatively slowly, as their up-regulated peaks appear at 3 dpi (five out of six instances). However, in the TBLN of pigs infected with PRV, PCV2 or PRRSV, the IFITM family members responsed more quickly and peaked at 1 dpi (four, six and five out of six instances for PRV, PCV2 and PRRSV, respectively). It is interesting that although the IFITM family transcriptome profile was repressed in response to SIV compared to the other viruses (with the possible exception of IFITM1), SIV was the only virus cleared by the pigs over the 14-day

duration of the experiment. The comparatively lower and slower up-regulation of most porcine IFITM genes in response to SIV infection as compared to the response to the other viruses may imply IFITMs were particularly targeted for suppression by SIV, indicating a rational feasibility for combating SIV through timely stimulation of porcine IFITM expression.

The ability of a virus to up-regulate the gene family differed. For each chart in Figure 4, we include the expression mean and its 95% confidence interval in the controls for each tag. PRV elicited the highest transcription levels, while PCV2 shows the weakest transcriptional activation by the IFITM family. Among a total of 24 instances (6 tags x 4 time-points), the PRV caused 9 instances of up-regulation by over 4-fold, while PCV2 produced a single instance with over 4-fold up-regulation. PRRSV also strongly stimulated high expression of the gene family, but the gene family reacted to SIV in a comparatively mild manner (Figure 4). However, SIV up-regulated *IFITM1* by 5.9 fold at day 3 post infection, the second highest to 6.5 fold at the same time-point with PRRSV infection.

Our current research revealed a limitation associated with the DGETP-based RNA-seq method, i.e., one tag can represent different genes/transcripts, particularly when gene family members have highly similar sequences. Our understanding is that RNA-seq cannot solve this problem either. The Illumina sequencing techniques usually produce sequences with a maximum of 100 bp in length. The highly conserved protein sequences shown in Figure 2 for several members of pig *IFITM* family are actually encoded by the

highly similar RNA molecules. As such, the same piece of the sequence provided by RNA-seq cannot be unequivocally assigned to any individual member in the gene family. In addition, the major drawbacks of whole transcriptome shotgun sequencing or RNA-seq include insufficient detection of genes/transcripts with low levels of expression, uneven sequencing depth along the length of a transcript and impossible usage of spreadsheet software for data processing due to large file size, (as reviewed by (Malone and Oliver, 2011). Our solution was to use different enzyme combinations and then identify a signature tag specifically for each member. For example, we found that a combination of four enzymes: *Tsp*509I (AATT), *Nla*III (CATG), *Msp*I (CCGG) and *Dpn*II (GATC) covered 99.64% of the *Sus scrofa* transcriptome.

3.4 Differentially expressed TBLN transcriptomes of pigs infected with SIV: an overview

Overall, we used a Bayesian framework approach and determined a total of 1,503 differentially expressed (DE) genes/transcripts in TBLN of pigs infected with SIV in the present study. Annotation of these DE genes/transcripts, based on their orthologous human counterparts, revealed a list of 1,286 functionally known genes. DAVID assigned 1,221 of them to 403 functional clusters. The top ten enriched functional clusters included genes associated with lysosomes (enrichment Score: 9.89), membrane-bounded vesicles (enrichment Score: 8.32), isopeptide bonds (enrichment Score: 6.10), apoptosis (enrichment Score: 5.95), regulation of apoptosis (enrichment Score: 5.71), inflammatory response (enrichment Score: 5.32), protein transport (Enrichment Score: 4.51), RNA binding and processing (enrichment Score: 4.28), protein biosynthesis (enrichment Score: 4.25) and the nucleoplasm (enrichment Score: 3.97).

Among the pig *IFITM* family members, only *IFITM1* and *IFITM3* were identified as DE genes in TBLN of pigs infected with SIV. Both members are involved in gene clusters as integral to membrane. In addition, *IFITM1* is also associated with the regulation of cell proliferation pathways involving 89 genes identified in the present study: NAMPT, NBN, AIF1, OSMR, TSG101, STAT5A, IL18, BTC, PPARG, NAP1L1, BAP1, SKAP2, TGFB1, CXCL10, S1PR2, MAGED1, MEN1, GPX1, CDCA7, GPC3, NDUFS4, CDKN2D, HMOX1, ILK, SERPINE1, SHC1, PDGFC, LTB, AKIRIN2, AGPAT1, MAP2K5, CTBP1, ARHGEF2, RBBP4, LYN, CD164, PPP1CB, MAPK1, TNS3, CD38, HHEX, BTG1, CD33, GRN, VEGFA, PDGFRB, ADAM17, EMP3, VSIG4, CNBP, CAV1, CCL2, LST1, *IFITM1*, GNAI2, PML, COMT, TIMP2, FTH1, CDH5, TIMP1, CD9, TSPAN31, CDC123, CAMK2D, TGM2, THBS1, LAMB1, PPAP2A, CD5, TXNIP, PTPRC, BECN1, PHB, ANXA1, DUSP22, SKI, IGF2, STAT1, CAPN1, CDC25B, PLA2G4A, CDKN1B, CCL14, HDAC1, FABP3, FABP4, HGS and ENG.

IFITM3 was assigned to an immune response pathway associated with 91 genes: NBN, IL27RA, IL16, IL18, PPARG, TLR1, TIRAP, PRDX2, TLR4, NFKB2, LY9, CXCL12, PRDX1, C1QC, TGFB1, CXCL10, CFP, LTB, FCGR3B, AKIRIN2, LAIR1, C5AR1, SIT1, BST2, LYN, LY96, SLA2, CNPY3, HLA-A, SERPING1, CD164, SIGIRR, C1QB, VEGFA, ADAM17, CTSC, MADCAM1, SEMA4D, VSIG4, LCP1, GBP1, YWHAZ, CCL2, LST1, HLA-DRB1, C3, IFITM3, TFE3, CXCL9, ACP5, CALCOCO2, OAS1, FCGRT, C1S, OAS2, FTH1, CCL26, SQSTM1, FCN1, FCER1G, C2, THBS1, DHX58, ARHGDIB, FYB, MSH6, PTPRC, ST6GAL1, CR2, SWAP70, CFB, SAMHD1,

CCL19, C4BPA, PSMB8, CD1D, CYBA, GPI, LAT, OASL, TNFSF10, CCL14, RGS1, FCGR2B, CXCL14, CXCL13, CD209, ANXA11, HSPD1, CD14 and IFI6.

As indicated above, *IFITM* family members responded to SIV, PRV, PCV2 and PRRSV differently. IAV belongs to the family of *Orthomyxoviridae* viruses. The pig is a natural host and a "mixing vessel" for IAV cross-species transmission particularly to humans (Ma et al., 2008; Vincent et al., 2008). Critically, influenza in pigs resembles influenza in humans: i) The same influenza A subtypes (H1 and H3) are predominately circulating and many are capable of causing disease in both human and swine populations; ii) Infected pigs display similar clinical symptoms as found in humans, such as fever, coughing, lethargy, anorexia and nasal discharge; iii) both species have a similar viral clearance phase of around 7-10 days. Therefore, the pig is a good mammalian model to study zoonotic influenza A virus (Kuiken et al., 2011; Ma and Richt, 2010; Torremorell et al., 2012). Although vaccines against influenza are available for humans and farm animals, it remains a challenge to control outbreaks of influenza infections because the virus evolves rapidly to evade host immunity through antigenic drift and shift. IFITMs are a group of transmembrane proteins that respond differentially to IFN induction and viral infections. Figure 6 shows the IFN-α_1 and IFN-β transcript abundance elevated at 3 dpi for PRRSV and PCV-2 (IFN-α_1 only), and at 1 and 14 dpi for IFN-β for PRV, as measured by RT-PCR in the TBLN of the infected pigs compared to controls. This IFN transcript data agrees with previous findings of a delayed or inhibited IFN response in PRRSV infection (Albina et al., 1998; Lee et al., 2004; Loving et al., 2007; Miller et al., 2004; Van Reeth et al., 1999). In the case of influenza A virus, the viral non-structural

protein 1 (NS1) has been described to act as a powerful antagonist of IFN induction (Hale et al., 2008) and this may explain why IFN-α/β transcript abundance was not elevated in the TBLN of the SIV-infected pigs. Alternatively, it is possible we do not detect high levels in the TBLN of SIV-infected pigs because induction of IFN-α/β usually occurs with 2 hr post-infection (Solorzano et al., 2005) and the peak transcript abundance may have been missed at our 1dpi time-point. Our data highlights that porcine IFITMs, the family of early response IFN-stimulated genes (ISGs) are part of the pig's antiviral response against influenza (Brass et al., 2009; Everitt et al., 2012; Huang et al., 2011).

This report presents the first description of the TBLN transcriptome responses of porcine *IFITM* and the genomic organization of the *IFITMs* in relation to the mouse and human genomes. These data indicate a need for more extensive transcriptional and functional characterization of porcine IFITMs, which will further our understanding of the IAV-host interaction and discovery of the host defense potential of IFITMs against pandemic SIV infection.

Acknowledgements

This work was supported in part by the National Pork Board Grant #08-247, the United States Department of Agriculture (USDA) Agricultural Research Service, and the Porcine Reproductive and Respiratory Syndrome Coordinated Agricultural Project USDA National Institute of Food and Agriculture Award 2008-55620-19132. We thank the following members of the Virus and Prion Research Unit at the National Animal Disease Center: A. Vincent, K. Faaberg and A.Cheung for providing the virus stock; J. Huegel and B. Pottenbaum for animal caretaking; and M. Baker (Iowa State University) M. Harland, D. Adolphson, S. Anderson, E. Zanella and A. Vorwald for technical assistance. Mention of trade names or commercial products in this article is solely for the purpose of providing specific information and does not imply recommendation or endorsement by the U.S. Department of Agriculture. USDA is an equal opportunity provider and employer.

Conflict of Interest

The authors have declared that no conflict of interest exists.

Ethics

The animal studies were reviewed and approved by the Institutional Animal Care and Use Committee (IACUC) of the National Animal Disease Center-USDA-Agricultural Research Service.

References

Albina, E., Carrat, C., Charley, B., 1998. Interferon-alpha response to swine arterivirus (PoAV), the porcine reproductive and respiratory syndrome virus. J Interferon Cytokine Res 18, 485-490.

Brass, A.L., Huang, I.C., Benita, Y., John, S.P., Krishnan, M.N., Feeley, E.M., Ryan, B.J., Weyer, J.L., van der Weyden, L., Fikrig, E., Adams, D.J., Xavier, R.J., Farzan, M., Elledge, S.J., 2009. The IFITM proteins mediate cellular resistance to influenza A H1N1 virus, West Nile virus, and dengue virus. Cell 139, 1243-1254.

Brockmeier, S., Halbur, P., Thacker, E., 2002. Porcine Respiratory Disease Complex, in: KA, B., JM, G. (Eds.), Polymicrobial Diseases. ASM Press, Washington (DC).

Brockmeier, S.L., Loving, C.L., Vorwald, A.C., Kehrli, M.E., Jr., Baker, R.B., Nicholson, T.L., Lager, K.M., Miller, L.C., Faaberg, K.S., 2012. Genomic sequence and virulence comparison of four Type 2 porcine reproductive and respiratory syndrome virus strains. Virus Res 169, 212-221.

Chou, K.C., Shen, H.B., 2010. A new method for predicting the subcellular localization of eukaryotic proteins with both single and multiple sites: Euk-mPLoc 2.0. PLoS One 5, e9931.

David, J.P., Coissac, E., Melodelima, C., Poupardin, R., Riaz, M.A., Chandor-Proust, A., Reynaud, S., 2010. Transcriptome response to pollutants and insecticides in the dengue vector Aedes aegypti using next-generation sequencing technology. BMC Genomics 11, 216.

Everitt, A.R., Clare, S., Pertel, T., John, S.P., Wash, R.S., Smith, S.E., Chin, C.R., Feeley, E.M., Sims, J.S., Adams, D.J., Wise, H.M., Kane, L., Goulding, D., Digard, P.,

Anttila, V., Baillie, J.K., Walsh, T.S., Hume, D.A., Palotie, A., Xue, Y., Colonna, V., Tyler-Smith, C., Dunning, J., Gordon, S.B., Smyth, R.L., Openshaw, P.J., Dougan, G., Brass, A.L., Kellam, P., 2012. IFITM3 restricts the morbidity and mortality associated with influenza. Nature 484, 519-523.

Gonzalez-Navajas, J.M., Lee, J., David, M., Raz, E., 2012. Immunomodulatory functions of type I interferons. Nat Rev Immunol 12, 125-135.

Groenen, M.A., Archibald, A.L., Uenishi, H., Tuggle, C.K., Takeuchi, Y., Rothschild, M.F., Rogel-Gaillard, C., Park, C., Milan, D., Megens, H.J., Li, S., Larkin, D.M., Kim, H., Frantz, L.A., Caccamo, M., Ahn, H., Aken, B.L., Anselmo, A., Anthon, C., Auvil, L., Badaoui, B., Beattie, C.W., Bendixen, C., Berman, D., Blecha, F., Blomberg, J., Bolund, L., Bosse, M., Botti, S., Bujie, Z., Bystrom, M., Capitanu, B., Carvalho-Silva, D., Chardon, P., Chen, C., Cheng, R., Choi, S.H., Chow, W., Clark, R.C., Clee, C., Crooijmans, R.P., Dawson, H.D., Dehais, P., De Sapio, F., Dibbits, B., Drou, N., Du, Z.Q., Eversole, K., Fadista, J., Fairley, S., Faraut, T., Faulkner, G.J., Fowler, K.E., Fredholm, M., Fritz, E., Gilbert, J.G., Giuffra, E., Gorodkin, J., Griffin, D.K., Harrow, J.L., Hayward, A., Howe, K., Hu, Z.L., Humphray, S.J., Hunt, T., Hornshoj, H., Jeon, J.T., Jern, P., Jones, M., Jurka, J., Kanamori, H., Kapetanovic, R., Kim, J., Kim, J.H., Kim, K.W., Kim, T.H., Larson, G., Lee, K., Lee, K.T., Leggett, R., Lewin, H.A., Li, Y., Liu, W., Loveland, J.E., Lu, Y., Lunney, J.K., Ma, J., Madsen, O., Mann, K., Matthews, L., McLaren, S., Morozumi, T., Murtaugh, M.P., Narayan, J., Nguyen, D.T., Ni, P., Oh, S.J., Onteru, S., Panitz, F., Park, E.W., Park, H.S., Pascal, G., Paudel, Y., Perez-Enciso, M., Ramirez-Gonzalez, R., Reecy, J.M., Rodriguez-Zas, S., Rohrer, G.A., Rund, L., Sang, Y., Schachtschneider, K., Schraiber, J.G., Schwartz, J., Scobie, L., Scott, C.,

Searle, S., Servin, B., Southey, B.R., Sperber, G., Stadler, P., Sweedler, J.V., Tafer, H., Thomsen, B., Wali, R., Wang, J., Wang, J., White, S., Xu, X., Yerle, M., Zhang, G., Zhang, J., Zhang, J., Zhao, S., Rogers, J., Churcher, C., Schook, L.B., 2012. Analyses of pig genomes provide insight into porcine demography and evolution. Nature 491, 393-398.

Hale, B.G., Randall, R.E., Ortin, J., Jackson, D., 2008. The multifunctional NS1 protein of influenza A viruses. J Gen Virol 89, 2359-2376.

Hickford, D., Frankenberg, S., Shaw, G., Renfree, M.B., 2012. Evolution of vertebrate interferon inducible transmembrane proteins. BMC Genomics 13, 155.

Huang da, W., Sherman, B.T., Tan, Q., Collins, J.R., Alvord, W.G., Roayaei, J., Stephens, R., Baseler, M.W., Lane, H.C., Lempicki, R.A., 2007. The DAVID Gene Functional Classification Tool: a novel biological module-centric algorithm to functionally analyze large gene lists. Genome biology 8, R183.

Huang, I.C., Bailey, C.C., Weyer, J.L., Radoshitzky, S.R., Becker, M.M., Chiang, J.J., Brass, A.L., Ahmed, A.A., Chi, X., Dong, L., Longobardi, L.E., Boltz, D., Kuhn, J.H., Elledge, S.J., Bavari, S., Denison, M.R., Choe, H., Farzan, M., 2011. Distinct patterns of IFITM-mediated restriction of filoviruses, SARS coronavirus, and influenza A virus. PLoS Pathog 7, e1001258.

Jiang, Z., Zhou, X., Michal, J.J., Wu, X.L., Zhang, L., Zhang, M., Ding, B., Liu, B., Manoranjan, V.S., Neill, J.D., Harhay, G.P., Kehrli, M.E., Jr., Miller, L.C., 2013. Reactomes of porcine alveolar macrophages infected with porcine reproductive and respiratory syndrome virus. PLoS One 8, e59229.

Katze, M.G., Fornek, J.L., Palermo, R.E., Walters, K.A., Korth, M.J., 2008. Innate immune modulation by RNA viruses: emerging insights from functional genomics. Nat Rev Immunol 8, 644-654.

Kuiken, T., Fouchier, R., Rimmelzwaan, G., van den Brand, J., van Riel, D., Osterhaus, A., 2011. Pigs, poultry, and pandemic influenza: how zoonotic pathogens threaten human health. Advances in experimental medicine and biology 719, 59-66.

Lager, K.M., Gauger, P.C., Vincent, A.L., Opriessnig, T., Kehrli, M.E., Jr., Cheung, A.K., 2007. Mortality in pigs given porcine circovirus type 2 subgroup 1 and 2 viruses derived from DNA clones. Vet Rec 161, 428-429.

Lee, S.M., Schommer, S.K., Kleiboeker, S.B., 2004. Porcine reproductive and respiratory syndrome virus field isolates differ in in vitro interferon phenotypes. Vet Immunol Immunopathol 102, 217-231.

Liu, S., Lin, L., Jiang, P., Wang, D., Xing, Y., 2011. A comparison of RNA-Seq and high-density exon array for detecting differential gene expression between closely related species. Nucleic Acids Res 39, 578-588.

Livak, K.J., Schmittgen, T.D., 2001. Analysis of relative gene expression data using real-time quantitative PCR and the 2(-Delta Delta C(T)) Method. Methods 25, 402-408.

Loving, C.L., Brockmeier, S.L., Sacco, R.E., 2007. Differential type I interferon activation and susceptibility of dendritic cell populations to porcine arterivirus. Immunology 120, 217-229.

Lu, J., Pan, Q., Rong, L., He, W., Liu, S.L., Liang, C., 2011. The IFITM proteins inhibit HIV-1 infection. Journal of virology 85, 2126-2137.

Ma, W., Kahn, R.E., Richt, J.A., 2008. The pig as a mixing vessel for influenza viruses: Human and veterinary implications. J Mol Genet Med 3, 158-166.

Ma, W., Richt, J.A., 2010. Swine influenza vaccines: current status and future perspectives. Anim Health Res Rev 11, 81-96.

Malone, J.H., Oliver, B., 2011. Microarrays, deep sequencing and the true measure of the transcriptome. BMC biology 9, 34.

Mann, M., Jensen, O.N., 2003. Proteomic analysis of post-translational modifications. Nature biotechnology 21, 255-261.

Marchler-Bauer, A., Zheng, C., Chitsaz, F., Derbyshire, M.K., Geer, L.Y., Geer, R.C., Gonzales, N.R., Gwadz, M., Hurwitz, D.I., Lanczycki, C.J., Lu, F., Lu, S., Marchler, G.H., Song, J.S., Thanki, N., Yamashita, R.A., Zhang, D., Bryant, S.H., 2013. CDD: conserved domains and protein three-dimensional structure. Nucleic Acids Res 41, D348-352.

Miller, L.C., Laegreid, W.W., Bono, J.L., Chitko-McKown, C.G., Fox, J.M., 2004. Interferon type I response in porcine reproductive and respiratory syndrome virus-infected MARC-145 cells. Arch Virol 149, 2453-2463.

Miller, L.C., Zanella, E.L., Waters, W.R., Lager, K.M., 2010. Cytokine protein expression levels in tracheobronchial lymph node homogenates of pigs infected with pseudorabies virus. Clin Vaccine Immunol 17, 728-734.

Pierleoni, A., Martelli, P.L., Casadio, R., 2011. MemLoci: predicting subcellular localization of membrane proteins in eukaryotes. Bioinformatics 27, 1224-1230.

Sallman Almen, M., Bringeland, N., Fredriksson, R., Schioth, H.B., 2012. The dispanins: a novel gene family of ancient origin that contains 14 human members. PLoS One 7, e31961.

Siegrist, F., Ebeling, M., Certa, U., 2011. The small interferon-induced transmembrane genes and proteins. Journal of interferon & cytokine research : the official journal of the International Society for Interferon and Cytokine Research 31, 183-197.

Solorzano, A., Webby, R.J., Lager, K.M., Janke, B.H., Garcia-Sastre, A., Richt, J.A., 2005. Mutations in the NS1 protein of swine influenza virus impair anti-interferon activity and confer attenuation in pigs. J Virol 79, 7535-7543.

Straw, B.E., 1999. Diseases of swine, 8th ed. Iowa State University Press, Ames, Iowa.

Tamura, K., Peterson, D., Peterson, N., Stecher, G., Nei, M., Kumar, S., 2011. MEGA5: molecular evolutionary genetics analysis using maximum likelihood, evolutionary distance, and maximum parsimony methods. Mol Biol Evol 28, 2731-2739.

Torremorell, M., Allerson, M., Corzo, C., Diaz, A., Gramer, M., 2012. Transmission of Influenza A Virus in Pigs. Transbound Emerg Dis.

Van Reeth, K., Labarque, G., Nauwynck, H., Pensaert, M., 1999. Differential production of proinflammatory cytokines in the pig lung during different respiratory virus infections: correlations with pathogenicity. Res Vet Sci 67, 47-52.

Vincent, A.L., Ma, W., Lager, K.M., Janke, B.H., Richt, J.A., 2008. Swine influenza viruses a North American perspective. Advances in virus research 72, 127-154.

Vincent, A.L., Swenson, S.L., Lager, K.M., Gauger, P.C., Loiacono, C., Zhang, Y., 2009. Characterization of an influenza A virus isolated from pigs during an outbreak of

respiratory disease in swine and people during a county fair in the United States. Veterinary Microbiology 137, 51-59.

Waterhouse, A.M., Procter, J.B., Martin, D.M., Clamp, M., Barton, G.J., 2009. Jalview Version 2--a multiple sequence alignment editor and analysis workbench. Bioinformatics 25, 1189-1191.

Yount, J.S., Moltedo, B., Yang, Y.Y., Charron, G., Moran, T.M., Lopez, C.B., Hang, H.C., 2010. Palmitoylome profiling reveals S-palmitoylation-dependent antiviral activity of IFITM3. Nat Chem Biol 6, 610-614.

Tables

Table 1. IFITM primers.

PCR primers	Sequence 5′–3′	Len.	Tm	Amplicon (bp)
F-IFITM1-197	CTTCTGACATCCAGACACAGC	21	59	295
R-IFITM1-491	GTCTCCCACCATCTTCCGGT (iden. to 2,3, lLs)	20	61	
F-IFITM2-128	CGGTGATCAACATCCGAAGCG (iden. to 3, 1L1, 1L2, 1L4 and 3L2)	21	62	253
F-IFITM2-380	ACAAACACCAGAAGAACAGTGGC (iden. to 1)	23	61	
F-IFITM3-173	TCTGGTCCCTGTTCAACACC (iden. to 1,2, 3Ls)	20	59	209
R-IFITM3-381	GCCAGTGGTGCAAACGATG	19	60	
F-IFITM1L1-384	ATGGTGGGAGACATCACTGG (iden. to 2, 1L3)	20	59	286
R-IFITM1L1-669	GAACCCAGTTGTGGACAGGT (iden. to 1)	20	59	
F-IFITM1L2-389	GGTGGGAGACATCATTGGGG	20	59	285
R-IFITM1L2-635	TGAACCCAGTTGTGGACAGG	20	60	
F-IFITM1L3-106	GGTTCAGCTCCCATGACCAG	20	60	276
R-IFITM1L3-381	TGCAAACACCAGAAGAGCGA (iden. to 1, 2, lLs)	20,	60	
F-IFITM1L4-473	GTCGCTCTTCTGGTGTTTGC	20	59	269
R-IFITM1L4-741	GGCGAGCCTGTAACTTCTCT	20	59	
F-IFITM5-195	CAAGGCCCGAGATCAGAAGG	20	60	204
R-IFITM5-398	GAGTCGTCGAACTTGGTGCT	20	60	
F-IFITM3L1-93	CCTTCTTCACTGGTGCCCAT	20	59	238
R-IFITM3L1-330	TCAGGGCCCACCTTCACG	18	61	
F-IFITM3L2-115	TGATCAAGAGCCAGCACGAG	20	60	197
R-IFITM3L2-311	GGGCATGGCCACCTTCA	17	59	

Table 2. Porcine IFITM gene locus and structures based on current swine genome assembly (Sscorfa 10.2).

Gene locus	Symbol	Chromosome coordinates	RefSeq	ISRE	Exon 1	Intron	Exon 2	ESTs
LOC100127358	IFITM1	SSC2: 162099157.162100564 (-)	XM_003124230.1	Yes	464	623	321	Yes
LOC100620056	IFITM2	SSC2: Gene ID: 100620056 (-)	NM_001246214.1	Yes	319	N/A	1219	Yes
LOC100518544	IFITM3	SSC2: 162072261.162072507 (-)	NM_001201382.1	Yes	247	419	192	Yes
LOC100627004	IFITM1L1 IFTIM1L2	SSC2: 162339710.162341038 (-)	XM_003354415.1	Yes	368	637	324	Yes
LOC100626247	(4 transcript variants)	SSC2: 162076668.162094496 (-)	XM_003354411.1	Yes	352 (v1)	289 (v1)	324 (v1)	Yes
LOC100621926	IFTIM1L3 (3 exons)	SSC1: 296319106.296331356 (+)	XM_003353647.2	Yes	40	1153	206	No
LOC100519082	IFTIM1L4	SSC2: 162095298.162097522 (+)	XM_003124235.2	Yes	358	636	1230	Yes
LOC100518184	IFITM5	SSC2: 162116292.162117532 (+)	XM_003124229.3	No	198	682	361	Yes
LOC100627180	IFITM5L	SSC2: 162317991.162319234 (-)	XM_003354416.2	No	201	682	361	Yes
LOC100627740	IFITM3L1 (partial)	SSC2: 162353100.162354440 (+)	XM_003354422.2	Yes	323	964	53	No
LOC100627649	IFITM3L2	SSC2: 162333055.162334436 (+)	XM_003354421.1	Yes	302	987	91	No

ISRE, interferon-stimulated response element in core promoter regions; ESTs, expressed sequence tags.

Table 3. Predicted subcellular localization of human and porcine IFITMs.

	Subcellular localization[a]		
	HslPred	Euk-mPLoc	BaCelLo
pIFITM1	CM	CM	MT
pIFITM2	CP	CM	CP
pIFITM3	CM	CM	CP
pIFITM1L1	CP	CM	MT
pIFITM1L2	CP	CM	MT
pIFITM1L3	CP	CM	EC
pIFITM1L4	CP	CM	MT
pIFITM3L1	CP	CM	CP
pIFITM3L2	MT	CM	EC
pIFITM5	CP	EC	CP
pIFITM5L	CP	EC	CP
hIFITM1	CM	CM	CP
hIFITM2	CM	CM	CP
hIFITM3	CM	CM	CP
hIFITM5	CP	EC. MT	CP

[a]Predicted with three programs for eukaryotic proteins using hybrid approach (Hslpred), or algorithms based on a decision tree of several support vector machines (Euk-mPloc and MemiLoci). CP, cytoplasmic protein; CM, cell membrane; EC, extracellular; MT, Mitochondrial protein.

Figures

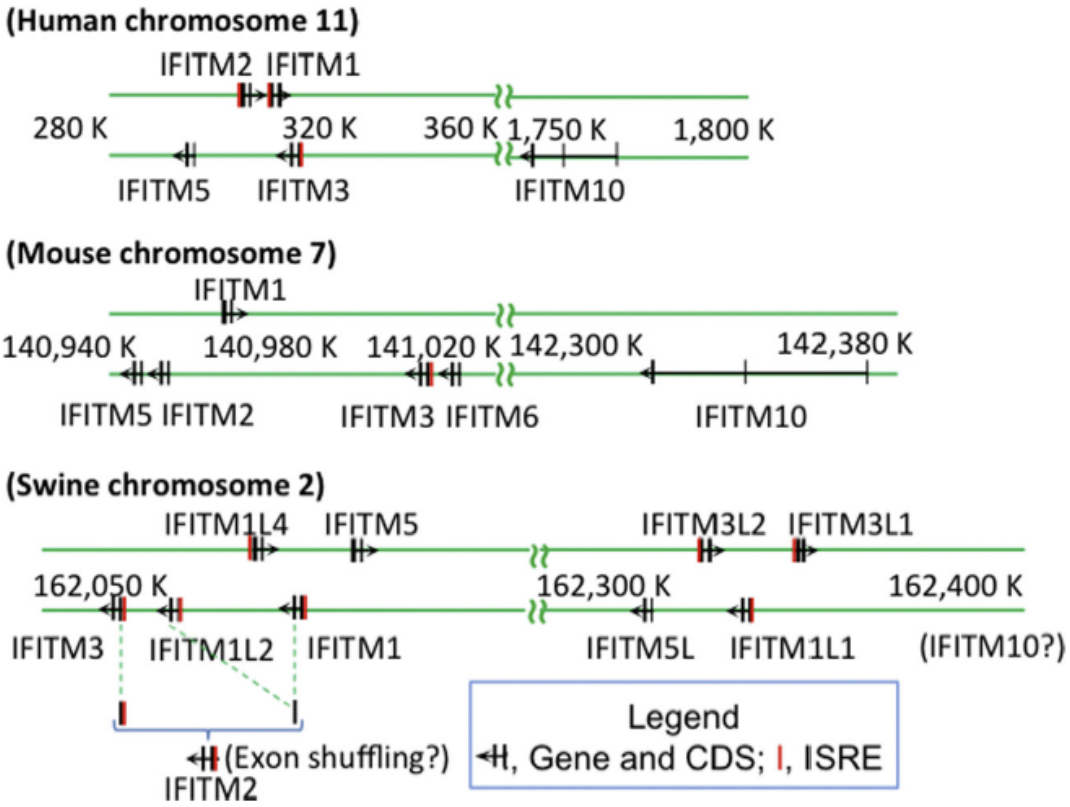

Figure 1. Chromosomal location of IFITM genes and the existence of interferon-stimulated response element (ISRE, red bars) in their putative proximal promoter region. Green lines represent two strands of chromosomal DNA and black vertical bars represent exons of IFITM genes with the orientation of transcription indicated by the arrows. Human and mouse IFITM gene information was adapted from Siegrist et al., 2011, with modification. A piece of sequence on an unplaced genomic scaffold (NW_003541064.1, Sscrofa10.2) was detected to show 100% identity to N-terminal ~160 nt of human *IFITM10*.

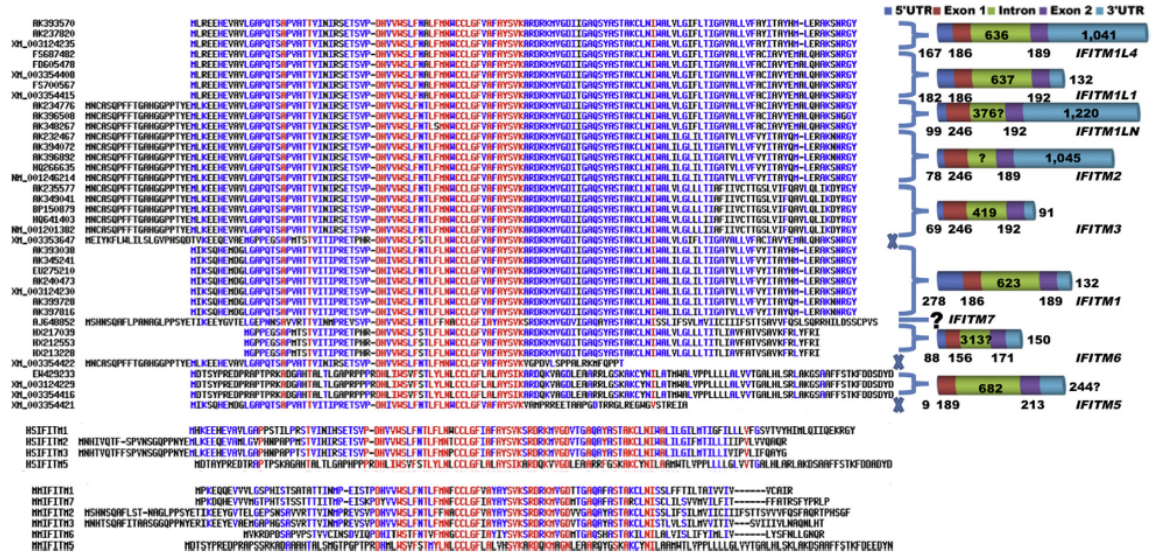

Figure 2. Annotation of IFITM family member in pigs with amino acid sequences and their genomic organizations. The 5'UTR, exon 1, intron, exon 2 and 3'UTR were proportionally drawn according to their actual sizes if known. "?' indicates a partially known region or a totally unknown region in size. "X" means that these model RefSeqs have no EST or non-RefSeq RNA evidence. Both human and mouse information are included.

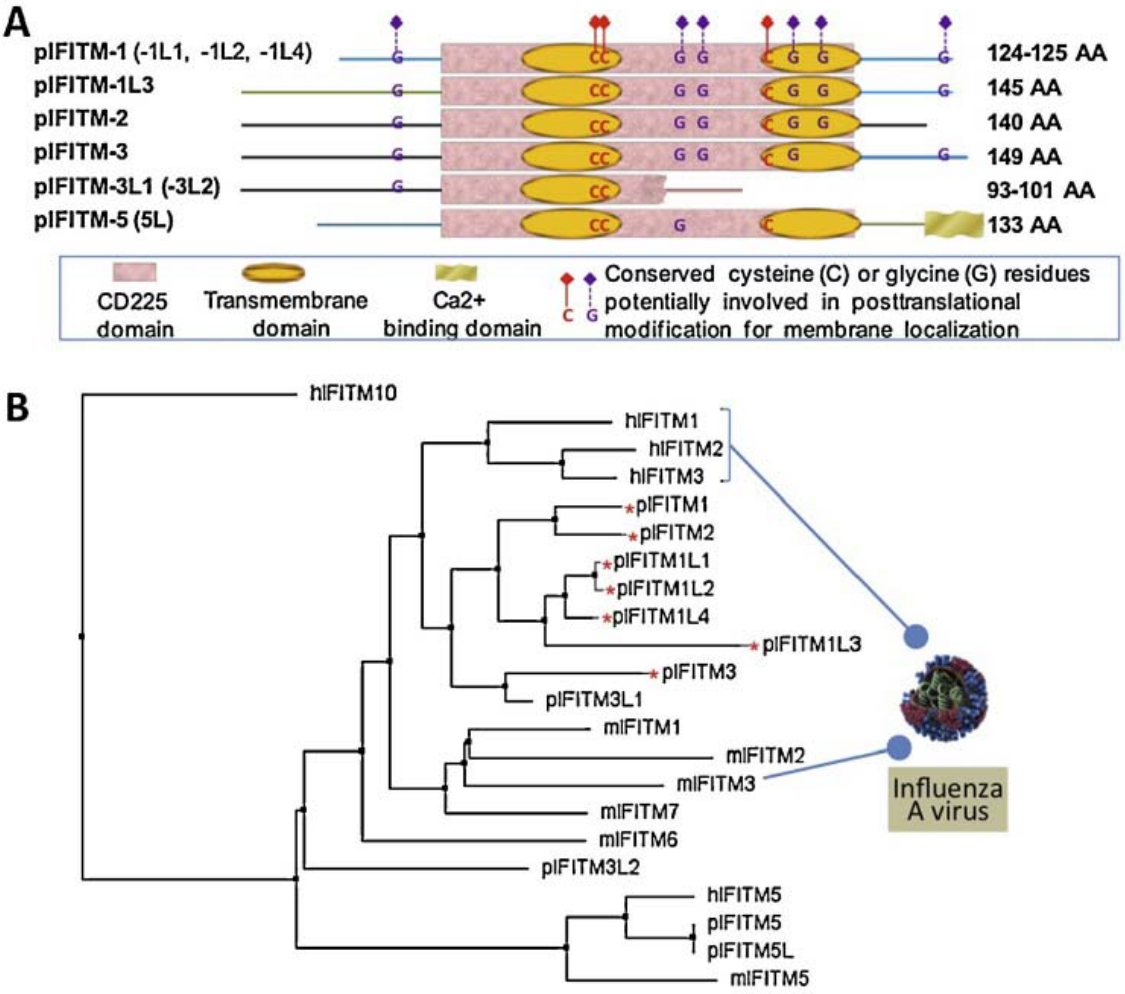

Figure 3. (A) Sequence and domain structure analyses of porcine IFITM proteins. All porcine IFITM proteins are centered by a CD225 functional domain of ~90 AA nearly flanked by two transmembrane (TM) domains, except the two IFITM3L1 and 3L2 having C-terminal truncated CD225 and only one TM domain. The diversity of N-terminal and C-terminal sequence among all isoforms is depicted with line fragments of different color and length**.** (B) Phylogenic analysis of human, mouse and porcine IFITM proteins rooted using human IFITM10. All IFITMs from the three species have been evolved from a closer ancestor than IFITM5 proteins that form into a separate ortholog cluster. The mammalian IFITM isoforms that have identified antiviral activity against influenza viruses are depicted with ball lines; and asterisks (*) label porcine IFITMs predictably to have anti-influenza activity. Species abbreviation: h, human; m, mouse and p, pig.

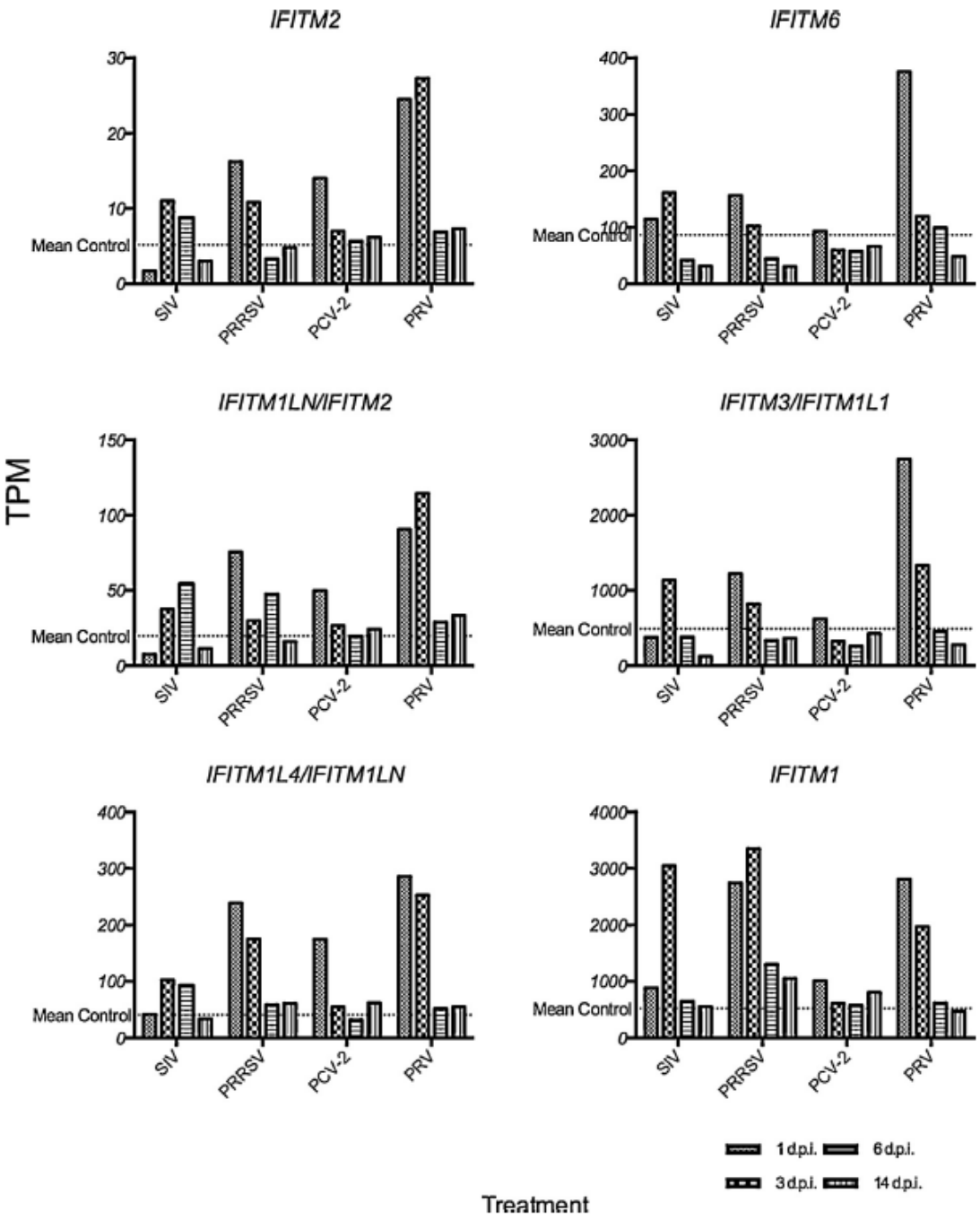

Figure 4. Expression dynamics of IFITM family members in TBLN samples from pigs infected with SIV, PRV, PCV2 and PRRSV at 1, 3, 6 and 14 dpi. Six porcine IFITM genes were transcribed, with IFITM1, IFITM3/IFITM1L1abundantly expressed and up-regulated at 3 dpi in the TBLN of SIV-infected pigs. , significantly different TPM (95% confidence interval) from control mean; IFITM, interferon induced transmembrane proteins; TPM, transcripts per million tags.

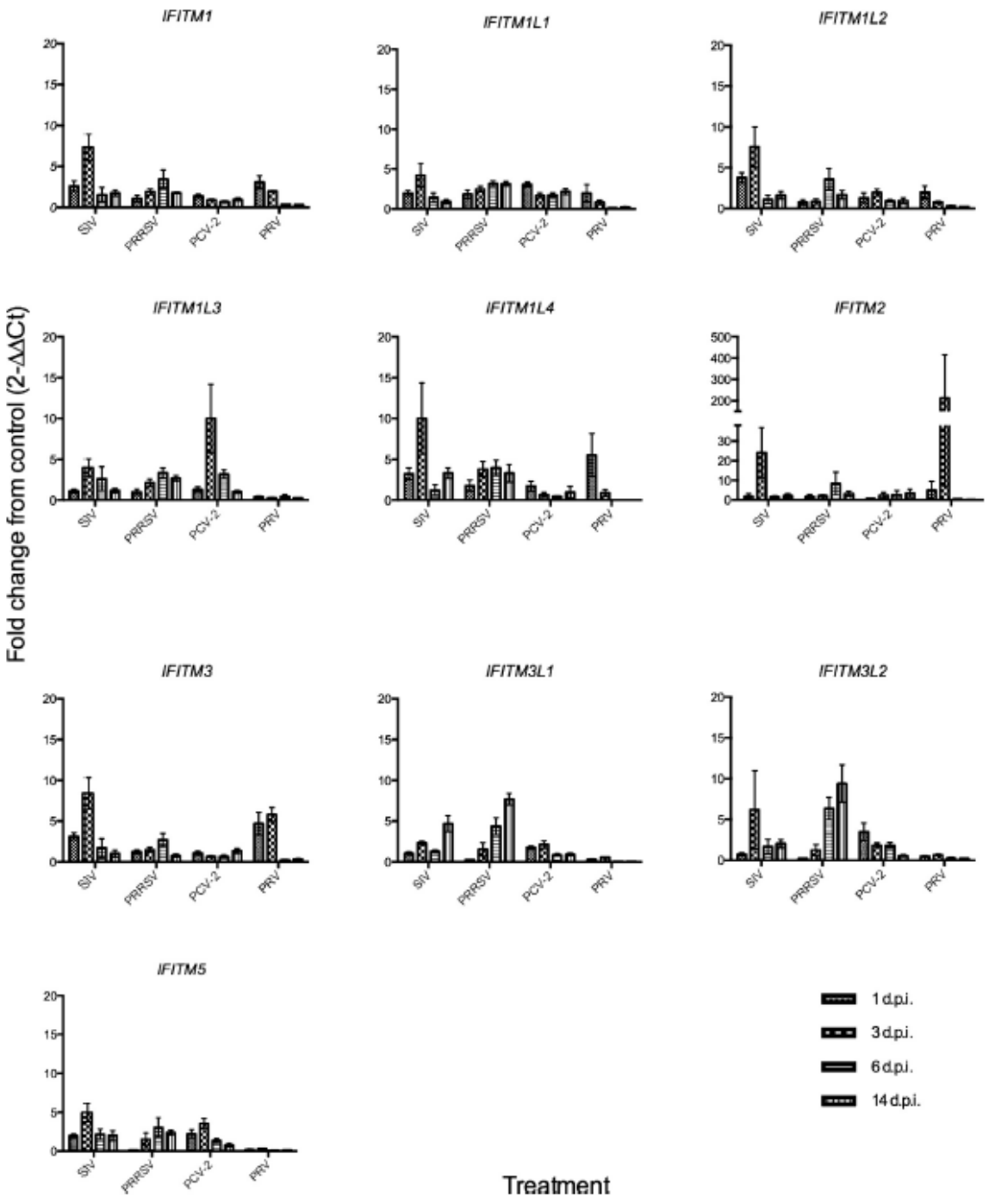

Figure 5. Real-time RT-PCR
Validation by real-time RT-PCR on RNA from the individual samples used in the DGETP analysis of selected IFITM transcripts showing differential transcript abundance. Fold change from the mean control transcript abundance ($2^{-\Delta\Delta Ct}$) (left *y* axis) are shown for transcripts *IFITM1*, *IFITM1L1*, *IFITM1L2*, *IFITM1L3*, *IFITM1L4*, *IFITM2*, *IFITM3*, *IFITM3L1*, *IFITM3L2* and *IFITM5* normalized to the 18S endogenous control.

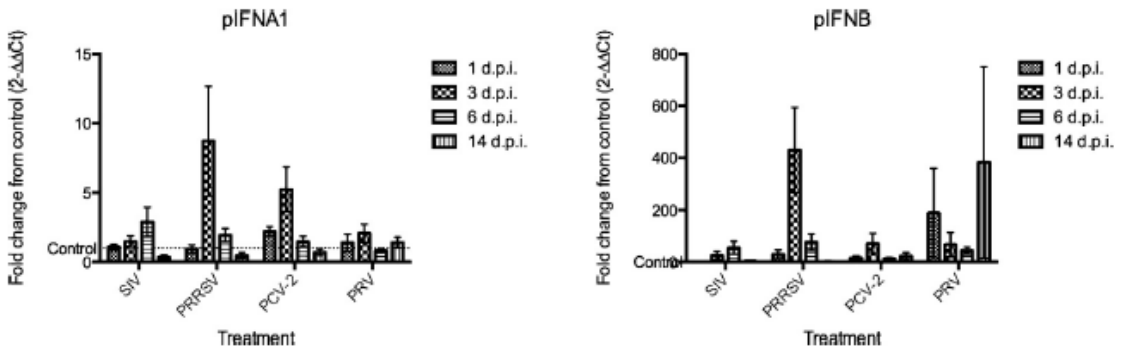

Figure 6. IFN-α_1 and IFN-β transcript abundance
Real-time RT-PCR on RNA from the individual samples used in the DGETP analysis of IFN-α_1 and IFN-β transcripts showing differential transcript abundance. Fold change from the mean control transcript abundance ($2^{-\Delta\Delta Ct}$) (left *y* axis) are shown for IFN-α_1 and IFN-β transcripts normalized to the 18S endogenous control.